Available online at www.sciencedirect.com
ScienceDirect
International Journal of Heat and Mass Transfer 51 (2008) 717–723
International Journal of HEAT and MASS TRANSFER
www.elsevier.com/locate/ijhmt

Mixed convection along a rotating vertical slender cylinder in an axial flow

Param Jeet Singh, S. Roy *

Department of Mathematics, Indian Institute of Technology Madras, Chennai 600 036, India

Received 10 October 2006
Available online 6 September 2007

Abstract

A general analysis has been developed to study fluid flow and heat transfer characteristics for mixed convection along a rotating vertical slender cylinder. Transformed set of coupled non-linear partial differential equations is solved by an implicit finite difference scheme in combination with the quasilinearisation technique. The effects of rotational, buoyancy and suction/injection parameters have been investigated in the present study. The effects of various parameters on the velocity profiles in x- and θ-directions and the temperature profile are reported in the present study. The buoyancy force causes considerable velocity overshoot for low Prandtl number (Pr) fluids. The Prandtl number (Pr) strongly affects the surface heat transfer rate. Numerical results are presented for the skin friction coefficients in x- and θ-directions and for the Nusselt number.

1. Introduction

The combination of free and forced convection (mixed convection) is encountered in many industrial and technological applications such as nuclear reactor cooled during emergency shutdown, solar central receiver exposed to wind current and heat exchanger placed in a low velocity environments etc. Mixed convection flow occurs when the free stream, inertial and near wall buoyant forces have strong effects on the convective heat transport. The system to be studied in the present investigation, shown schematically in Fig. 1, is a rotating vertical slender cylinder in a viscous fluid when the axis of the slender cylinder is inline with the flow. If the cylinder surface and free stream temperature differs, not only energy will be transferred to the flow but also density difference exists. In a gravitational field this density difference result in an additional force, buoyancy force, beside viscous force due to viscous action. In many practical situations of moderate flow velocities and large fluid wall temperature difference, the magnitude of buoyancy force and viscous force are of comparable order and convective heat transfer process is considered as mixed convection. Flow over cylinder considered as two dimensional as the cylinder radius is large compared to the boundary layer thickness and if the cylinder radius is of the order of the boundary layer thickness then the flow is considered as axi-symmetric. The radius of the slender cylinder is same as the order of the boundary layer thickness. Therefore, the flow considered as axi-symmetric instead of two dimensional. The nature of the flow on a slender cylinder is much characterized by its two surface curvatures, the longitudinal one in the meridian plane and the transverse one in the plane normal to the axis of symmetry.The first quantity is associated with any curved surface that causes centrifugal force in the flow. In the boundary layer analysis, longitudinal curvature is assumed to be very small compared to unity. Therefore, the effect of longitudinal curvature effect is negligible. In the axi-symmetric flow, the governing equations contains the transverse curvature term which influence the velocity and

* Corresponding author. Tel.: +91 044 2257 8492; fax: +91 044 2257 4602.
E-mail addresses: paramjeet@iitm.ac.in (P.J. Singh), sjroy@iitm.ac.in (S. Roy).
URL: http://mat.iitm.ac.in/sat.html (S. Roy).

0017-9310/$ - see front matter © 2007 Elsevier Ltd. All rights reserved.
doi:10.1016/j.ijheatmasstransfer.2007.04.053

Nomenclature

Roman letters

A	surface mass transfer parameter
C_{fx}	local skin friction coefficient in x-direction
$C_{f\theta}$	local skin friction coefficient in θ-direction
f	dimensionless stream function
g	dimensionless temperature
g^*	acceleration due to gravity
Gr_x	local Grashof number
k	thermal conductivity
Nu_x	local Nusselt number
Pr	Prandtl number
r_0	radius of cylinder
r	radial co-ordinate
Re	reference Reynolds number
Re_x	Reynolds number
s	dimensionless angular velocity
T	temperature
u	axial velocity component
v	radial velocity component
x	axial co-ordinate

Greek symbols

α	thermal diffusivity
η	similarity variable
λ	buoyancy parameter
λ_1	rotational parameter
μ	dynamic viscosity
ν	kinematic viscosity
ξ	transverse curvature
ρ	density
ψ	dimensionless stream function

Subscripts

w, ∞	conditions at the wall and infinity, respectively
ξ, η	denote the partial derivatives w.r.t these variables, respectively.

temperature fields. The impact of transverse curvature is important in several applications such as wire and fibre drawing where accurate prediction is required and thick boundary layer can exist on slender or near slender bodies. Chen and Mucoglu [1] were the first to study the slender cylinder problem for a uniform wall temperature case. In this case the solutions of the governing boundary layer equations was obtained by local non-similarity method.

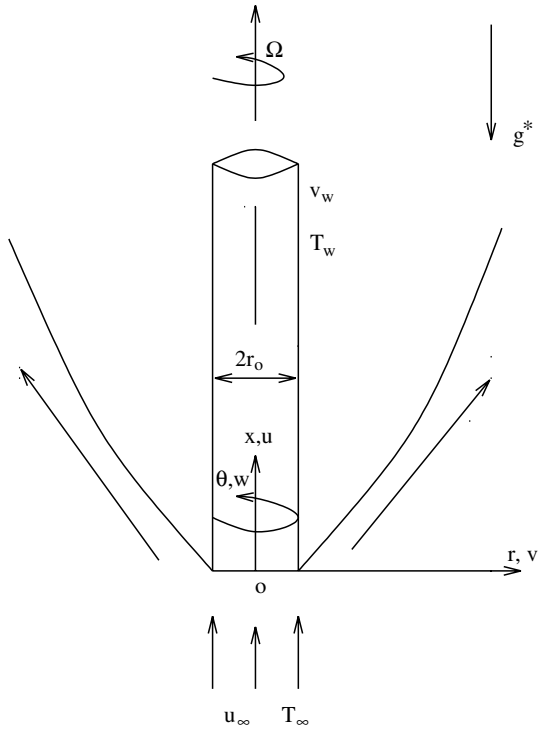

Fig. 1. Physical model and co-ordinate system.

Later, Naraian [2] dealt with the problem of combined free and forced convection heat transfer over a vertical slender cylinder in a uniform stream with isothermal walls. Subsequently, Bui and Cebeci [3] and Wang and Kleinstrever [4] considered the same problem for the case of uniform wall temperature and solved the governing boundary layer equations by using a finite difference scheme based on the central difference scheme. Mixed convection along slender vertical cylinder with variable surface temperature was studied by Heckel et al. [5]. They analyzed the case of the surface temperature $T_w(x)$ varies arbitrarily with the axial co-ordinate x and covered the entire mixed convection regime from pure free convection to pure forced convection. Later, Takhar et al. [6] studied the combined heat and mass transfer along a vertical moving cylinder with a free stream for both uniform wall temperature and uniform heat flux. Recently, Kumari and Nath [7] analyzed the effects of localized cooling/heating and suction/injection on the mixed convection flow on a thin vertical cylinder. In the brief literature, it is understood that the earlier investigation have not studied the influence of rotation on a mixed convection flow along a slender cylinder.

The aim of the present study is to investigate the suction/injection, rotation and transverse curvature effects on the mixed convection flow along a vertical slender cylinder. Several transport processes with surface mass transfer, i.e., injection (or suction) in industry where thermal diffusion caused by temperature gradient, such as polymer fiber coating or the coating of wires etc., may have useful application in the present study. In these applications, the careful control of yarn-quenching temperature or the heating and cooling temperature has a strong bearing on the final product quality [8]. The non-similar solution of the coupled non-linear partial differential equations governing the

mixed convection flow has been obtained numerically using the quasi-linearization technique in combination with the implicit finite difference scheme. The results for some particular cases are matched with Chen and Mucoglu [1] and Takhar et al. [6] for the uniform wall temperature (UWT) and found them in excellent agreement.

2. Analysis

Consider the steady mixed convection flow over a rotating vertical slender cylinder. The physical model and co-ordinate system are shown in Fig. 1. The radius of the cylinder is r_0 and the temperature at the wall vary as a function of x. The radial co-ordinate r is measured from the axis of the cylinder and the axial co-ordinate x is measured vertically upward such as $x = 0$ corresponds to the leading edge. The radius of the slender cylinder is same as the order of the boundary layer thickness. Therefore, the flow considered as axi-symmetric. Thermophysical properties of the fluid in the flow model are assumed to be constant except the density variations causing a body force term in momentum equation. The Boussinesq approximation is invoked for the fluid properties to relate density changes to temperature changes, and to couple in this way the temperature field to the flow field [9]. Under the above assumptions, the equations of conservation of mass, momentum and energy governing the mixed convection boundary layer flow over a rotating vertical slender cylinder can be expressed as:

$$\frac{\partial u}{\partial x}+\frac{1}{r}\frac{\partial (rv)}{\partial r}=0, \tag{1}$$

$$u\frac{\partial u}{\partial x}+v\frac{\partial u}{\partial r}-\frac{w^2}{r}=\frac{v}{r}\frac{\partial}{\partial r}\left(r\frac{\partial u}{\partial r}\right)+g^*\beta(T-T_\infty), \tag{2}$$

$$u\frac{\partial w}{\partial x}+v\frac{\partial w}{\partial r}+\frac{uw}{r}=\frac{v}{r}\frac{\partial}{\partial r}\left(r\frac{\partial w}{\partial r}\right), \tag{3}$$

$$u\frac{\partial T}{\partial x}+v\frac{\partial T}{\partial r}=\frac{\alpha}{r}\frac{\partial}{\partial r}\left(r\frac{\partial T}{\partial r}\right). \tag{4}$$

The boundary conditions are given by

$$\begin{aligned} &u(x,r_0)=0,\ v(x,r_0)=v_w,\ w(x,r_0)=\Omega r_0,\ T(x,r_0)=T_w(x),\\ &u(x,\infty)=u_\infty,\ w(x,\infty)=0,\ T(x,\infty)=T_\infty. \end{aligned} \tag{5}$$

Applying the following transformations:

$$\begin{aligned} &\xi=\left(\frac{4}{r_0}\right)\left(\frac{vx}{u_\infty}\right)^{\frac{1}{2}},\ \eta=\left(\frac{vx}{u_\infty}\right)^{-\frac{1}{2}}\left[\frac{r^2-r_0^2}{4r_0}\right],\ \frac{r^2}{r_0^2}=[1+\xi\eta],\\ &s=\frac{w}{r_0\Omega},\ u=\frac{1}{r}\frac{\partial\psi}{\partial r},\ v=-\frac{1}{r}\frac{\partial\psi}{\partial x},\ \psi(x,r)=r_0(vu_\infty x)^{\frac{1}{2}}f(\xi,\eta),\\ &g(\xi,\eta)=\frac{T-T_\infty}{T_w(x)-T_\infty},\ (T_w(x)-T_\infty)=(T_{w0}-T_\infty)\frac{r_0}{x},\\ &\lambda_1=\left(\frac{r_0\Omega}{u_\infty}\right)^2, \end{aligned}$$

$$\begin{aligned} &u=\frac{1}{2}u_\infty f_\eta(\xi,\eta),\ v=\frac{1}{2r}r_0\left(\frac{vu_\infty}{x}\right)^{\frac{1}{2}}(\eta f_\eta-f-\xi f_\xi),\\ &Re=\frac{u_\infty r_0}{v},Pr=\frac{v}{\alpha},\ Re_x=\frac{u_\infty x}{v},\ Gr_x=\frac{g^*\beta x^3(T_w(x)-T_\infty)}{v^2},\\ &\lambda=\frac{Gr_x}{Re_x^2}, \end{aligned} \tag{6}$$

to Eqs. (1)–(4) we find that Eq. (1) is satisfied identically, and Eqs. (2)–(4) reduce to

$$\begin{aligned} &(1+\xi\eta)f_{\eta\eta\eta}+(\xi+f)f_{\eta\eta}+8\lambda g+\frac{\xi^2\lambda_1 Res^2}{2(1+\xi\eta)^{1/2}}\\ &\quad=\xi\left(f_\eta\frac{\partial f_\eta}{\partial\xi}-f_{\eta\eta}\frac{\partial f}{\partial\xi}\right), \end{aligned} \tag{7}$$

$$\begin{aligned} &(1+\xi\eta)s_{\eta\eta}+(\xi+f)s_\eta-\frac{\xi^2 Re}{8(1+\xi\eta)^{1/2}}f_\eta s\\ &\quad=\xi\left(f_\eta\frac{\partial s}{\partial\xi}-s_\eta\frac{\partial f}{\partial\xi}\right), \end{aligned} \tag{8}$$

$$\begin{aligned} &Pr^{-1}(1+\xi\eta)g_{\eta\eta}+(\xi Pr^{-1}+f)g_\eta-2f_\eta g\\ &\quad=\xi\left(f_\eta\frac{\partial g}{\partial\xi}-g_\eta\frac{\partial f}{\partial\xi}\right). \end{aligned} \tag{9}$$

The boundary conditions reduce to

$$\begin{aligned} &f_\eta(\xi,0)=0,\ s(\xi,0)=1,\ g(\xi,0)=1,\quad \text{at } \eta=0,\\ &f_\eta(\xi,\eta_\infty)=2,\ s(\xi,\eta_\infty)=0,\ g(\xi,\eta_\infty)=0\quad \text{at } \eta=\eta_\infty, \end{aligned} \tag{10}$$

where

$$f(\xi,0)=-\frac{r_0 v_w\xi}{4v}=A\xi,\ A=-\frac{r_0 v_w}{4v}=\text{Constant}.$$

Here $A>0$ or $A<0$ corresponds to the suction or injection, respectively; ξ, η are the transformed co-ordinates; η_∞ is the edge of the boundary layer; Subscripts ∞ and w denote the conditions at the free stream and at the wall, respectively; the subscript η denotes the derivative with respect to η.

The local skin friction coefficient in x-direction is given by

$$C_{fx}=\frac{2\left[\mu\frac{\partial u}{\partial r}\right]_{r=r_0}}{\rho u_\infty^2}=2^{-1}(Re_x)^{-\frac{1}{2}}f_{\eta\eta}(\xi,0).$$

Thus,

$$Re_x^{\frac{1}{2}}C_{fx}=2^{-1}f_{\eta\eta}(\xi,0). \tag{11}$$

The local skin friction coefficient in θ-direction due to the rotational component of the velocity is given by

$$C_{f\theta}=\frac{2\left[\mu\frac{\partial w}{\partial r}\right]_{r=r_0}}{\rho u_\infty^2}=-(Re_x)^{-\frac{1}{2}}\lambda_1^{1/2}s_\eta(\xi,0).$$

Thus,

$$Re_x^{\frac{1}{2}}C_{f\theta}=-\lambda_1^{1/2}s_\eta(\xi,0). \tag{12}$$

The local heat transfer rate at the wall in terms of local Nusselt number can be expressed as:

$$Re_x^{-\frac{1}{2}} Nu_x = -2^{-1} g_\eta(\xi, 0), \tag{13}$$

where $Nu_x = -\dfrac{\left[x\left(\dfrac{\partial T}{\partial r}\right)\right]_{r=r_0}}{T_w - T_\infty}$.

3. Method of solution

The non-linear coupled partial differential equations (7)–(9) under the boundary conditions (10) have been solved numerically using an implicit finite difference scheme in combination with the quasi-linearization technique [10]. An iterative sequence of linear equations are carefully constructed to approximate the non-linear equations (7)–(9) for achieving quadratic convergence and monotonicity. Applying quasilinearization technique, the non-linear coupled partial differential equations (7)–(9) with boundary conditions (10) are replaced by the following sequence of linear partial differential equations.

$$f_{\eta\eta\eta}^{i+1} + A_1^i f_{\eta\eta}^{i+1} + A_2^i f_\eta^{i+1} + A_3^i f_{\eta\xi}^{i+1} + A_4^i s^{i+1} + A_5^i g^{i+1} = A_6^i, \tag{14}$$

$$s_{\eta\eta}^{i+1} + B_1^i s_\eta^{i+1} + B_2^i s^{i+1} + B_3^i s_\xi^{i+1} + B_4^i f_\eta^{i+1} + B_5^i g^{i+1} = B_6^i, \tag{15}$$

$$g_{\eta\eta}^{i+1} + C_1^i g_\eta^{i+1} + C_2^i g^{i+1} + C_3^i g_\xi^{i+1} + C_4^i f_\eta^{i+1} + C_5^i s^{i+1} = C_6^i. \tag{16}$$

The co-efficient function with iterative index i are known and the functions with iterative index $(i+1)$ are to be determined.The boundary conditions are given by

$$\begin{aligned} f_\eta^{i+1} &= 0, \quad s^{i+1} = g^{i+1} = 1 \quad \text{at } \eta = 0, \\ f_\eta^{i+1} &= 2, \quad s^{i+1} = g^{i+1} = 0, \quad \text{at } \eta = \eta_\infty. \end{aligned} \tag{17}$$

Since the method is described for ordinary differential equations by Inouye and Tate [11] and also explained for partial differential equations in a recent study by Roy and Saikrishnan [12], its detailed description is not provided for the sake of brevity. At each iteration step, the sequence of linear partial differential equations (14)–(16) were expressed in difference form using central difference scheme in the η-direction and backward difference scheme in ξ-direction. Thus, in each iteration step, the resulting equations were then reduced to a system of linear algebraic equations with a block tri-diagonal matrix, which is solved by Varga's algorithm [13]. To ensure the convergence of the numerical solution to the exact solution, the step sizes $\Delta\eta$ and $\Delta\xi$ have been optimized and taken as 0.01 and 0.01, respectively. The results presented here are independent of the step sizes at least up to the fourth decimal place. A convergence criterion based on the relative difference between the current and previous iteration values is employed. When the difference reaches 10^{-4}, the solution is assumed to have converged and the iterative process is terminated.

4. Result and discussion

Computations have been carried out for various values of $Pr(0.7 \leqslant Pr \leqslant 7.0)$, $A(-1.0 \leqslant A \leqslant 1.0)$, $\lambda(-4.0 \leqslant \lambda \leqslant 10.0)$ and $\lambda_1(0.0 \leqslant \lambda_1 \leqslant 5.0)$. The value of reference Reynolds number (Re) is taken as 10^4 for all numerical computations. The edge of the boundary layer (η_∞) has been taken between 3 and 5 depending on the values of the parameters. To verify our methods, we have compared our results with Chen and Mucoglu [1] and Takhar et al. [6] for the uniform wall temperature. The results are found in excellent agreement and some of the comparisons are shown in Table 1.

The effects of buoyancy parameter (λ) and Prandtl number (Pr) on the velocity and temperature profile (f_η, g) are displayed in Fig. 2. In buoyancy aiding flow ($\lambda > 0$), the buoyancy force shows the significant overshoot in the velocity profiles near the wall for lower Prandtl number fluid but for higher Prandtl number fluid the velocity overshoot is not present. The magnitude of the overshoot increases with the buoyancy parameter $\lambda(\lambda > 0)$ but decreases as the Prandtl number increases. The reason is that the buoyancy force (λ) affects more in low Prandtl number fluid (Air, $Pr = 0.7$) due to the low viscosity of the fluid, which increases the velocity within the boundary layer as the assisting buoyancy force acts like a favorable pressure gradient. Hence the velocity overshoot occurs and for higher Prandtl number fluids the overshoot is not much significant because higher Prandtl number (Water, $Pr = 7.0$) implies more viscous fluid which makes it less sensitive to the buoyancy parameter (λ). It is interesting to notice in Fig. 2 that at $\xi = 0.5$, for buoyancy opposing

Table 1
Comparison of results ($f_{\eta\eta}(\xi,0)$, $-g_\eta(\xi,0)$) for uniform wall temperature (UWT) case when rotational parameter $\lambda_1 = 0$ and $Pr = 0.7$ with those of Chen and Mucoglu [1] and Takhar et al. [6]

ξ	λ	Present results		Chen and Mucoglu [1]		Takhar et al. [6]	
		$f_{\eta\eta}(\xi,0)$	$-g_\eta(\xi,0)$	$f_{\eta\eta}(\xi,0)$	$-g_\eta(\xi,0)$	$f_{\eta\eta}(\xi,0)$	$-g_\eta(\xi,0)$
0	0	1.3281	0.5854	1.3282	0.5854	1.3281	0.5854
0	1	4.9665	0.8221	4.9666	0.8221	4.9663	0.8219
0	2	7.7124	0.9303	7.7126	0.9305	7.7119	0.9302
1	0	1.9168	0.8668	1.9172	0.8669	1.9167	0.8666
1	1	5.2580	1.0618	5.2584	1.0621	5.2578	1.0617
1	2	7.8870	1.1692	7.8871	1.1690	7.8863	1.1685

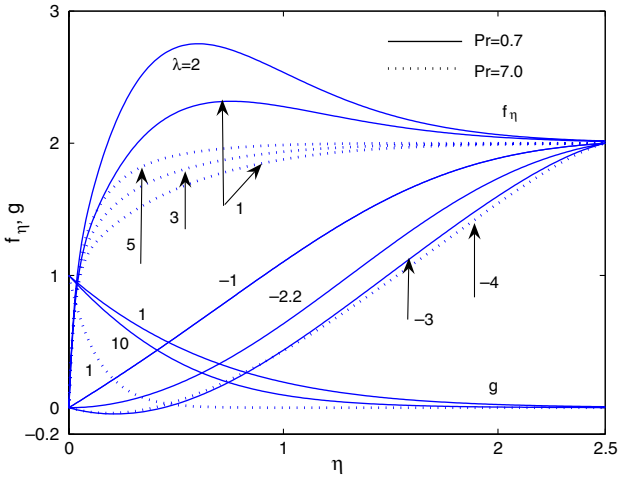

Fig. 2. Effects of λ and Pr on the velocity and temperature profiles (f_η, g) when $\lambda_1 = 1$, $A = 1$ and $Re = 10^4$ at $\xi = 0.5$.

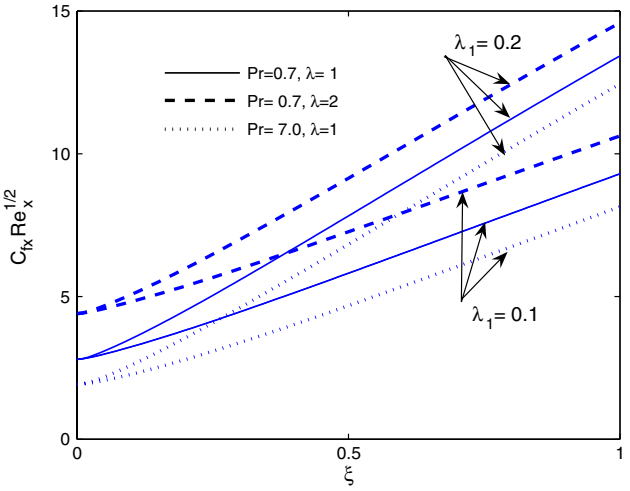

Fig. 4. Effects of λ, λ_1 and Pr on the skin friction coefficient $(C_{fx}Re_x^{1/2})$ when $A = 1$ and $Re = 10^4$.

flow, i.e., for negative value of buoyancy parameter $\lambda(\lambda < 0)$, the reverse flow starts at $\lambda \simeq -2.2$ for $Pr = 0.7$ (air) and at $\lambda \simeq -3.3$ for $Pr = 7.0$ (water). The buoyancy opposing force reduce the velocity near the wall subsequently as the buoyancy parameter λ decreases further and fluid flows backward near the wall in a small region as can be seen in Fig. 2 for $\lambda = -3$ when $Pr = 0.7$ and for $\lambda = -4$ for $Pr = 7.0$. The effect of λ is comparatively less in temperature profile as shown in Fig. 2. Moreover, Fig. 2 also shows that the effect of Prandtl number (Pr) results into the thinner thermal boundary layer as the higher Prandtl number (Water, $Pr = 7.0$) has a lower thermal conductivity. The effects of buoyancy parameter (λ) and rotation parameter (λ_1) on the angular velocity profile (s) are shown in Fig. 3. The effects of Prandtl number (Pr), buoyancy parameter (λ) and rotation parameter (λ_1) on skin friction coefficients $(C_{fx}Re_x^{1/2}, C_{f\theta}Re_x^{1/2})$ are shown in Figs. 4 and 5. The skin friction coefficients increase as the

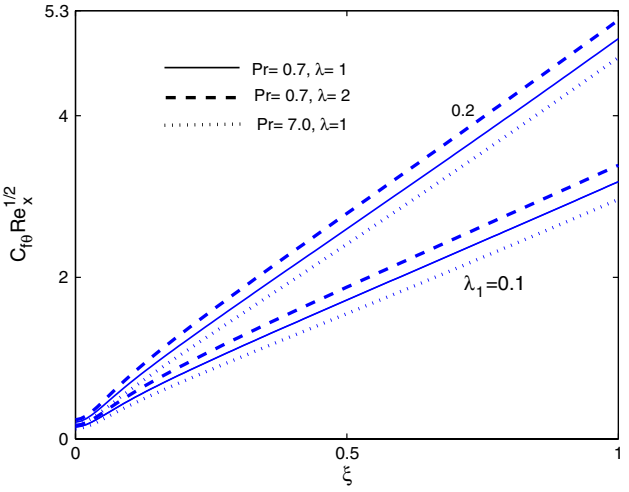

Fig. 5. Effects of λ, λ_1 and Pr on the skin friction coefficient $(C_{f\theta}Re_x^{1/2})$ when $A = 1$ and $Re = 10^4$.

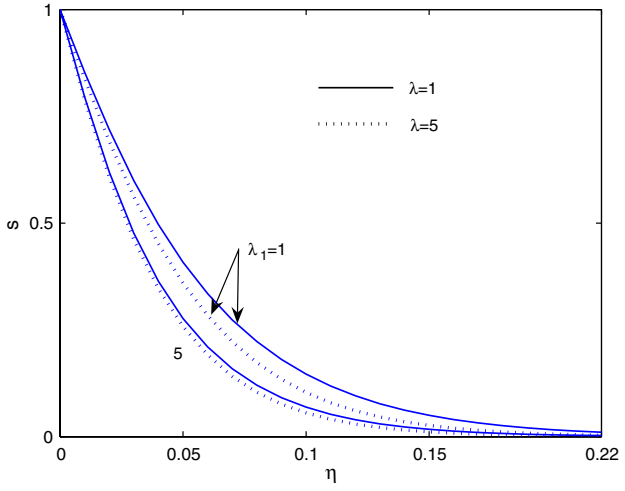

Fig. 3. Effects of λ and λ_1 on the angular velocity profile (s) when $A = 1$, $Pr = 0.7$ and $Re = 10^4$ at $\xi = 0.5$.

slender cylinder rotates faster, i.e., as the rotation parameter increases. This is because of the fact that as the slender cylinder rotates faster, it drags more fluid near the wall and consequently velocity gradient increases. Effect of λ_1 at $\xi = 0$ vanishes because of the fact that λ_1 is multiplied by ξ in the x-momentum equation. In particular, for $\lambda = 1$, $Pr = 0.7$, $A = 1$ and $\xi = 1$, Figs. 4 and 5 show that the percentage increase in the skin friction coefficients $(C_{fx}Re_x^{1/2}, C_{f\theta}Re_x^{1/2})$ for the increase of $\lambda_1 = 0.1$ to 0.2 are approximately 40% and 70%, respectively. It is also observed that the skin friction coefficients $(C_{fx}Re_x^{1/2}, C_{f\theta}Re_x^{1/2})$ increases with the increase of buoyancy parameter (λ). The physical reason is that positive buoyancy force ($\lambda > 0$) acts as a favorable pressure gradient, and fluid gets accelerated, which result in thinner momentum boundary layer. It is also found that the skin friction coefficients decrease with the increase of the Prandtl number. Because the higher Prandtl number means more viscous fluid, which

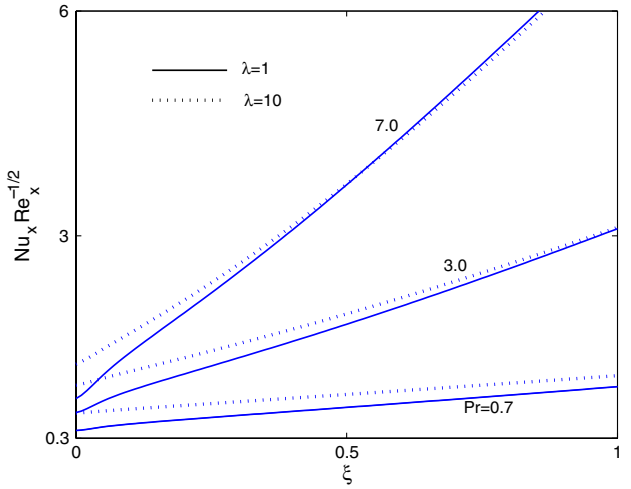

Fig. 6. Effects of λ and Pr on the Nusselt number $(Nu_x Re_x^{-1/2})$ when $A = 1$, $\lambda_1 = 1$ and $Re = 10^4$.

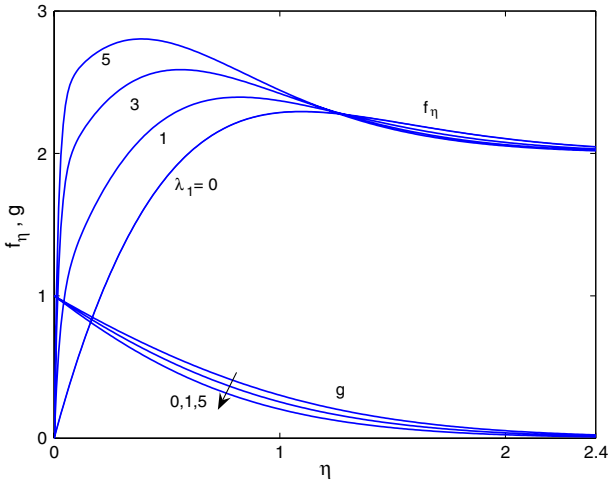

Fig. 7. Effect of λ_1 on the velocity and temperature profiles (f_η, g) when $\lambda = 1$, $A = 0$, $Re = 10^4$ and $Pr = 0.7$ at $\xi = 0.5$.

increase the boundary layer thickness and, consequently, reduce the shear stress.

The effects of Prandtl number (Pr) and buoyancy parameter (λ) on heat transfer coefficient $(Nu_x Re_x^{-1/2})$ are shown in Fig. 6. Prandtl number affects more profoundly on heat transfer coefficients as compared to the buoyancy parameter (λ). Fig. 6 reveals that the surface heat transfer rate increases significantly with Prandtl number (Pr) as the higher Prandtl number fluid has a lower thermal conductivity, which results in the thinner thermal boundary layer and, hence a higher heat transfer rate at the wall. It is also observed that the heat transfer coefficient $(Nu_x Re_x^{-1/2})$ increases with the increase of buoyancy parameter (λ). Fig. 6 shows that the percentage increase in the heat transfer coefficient $(Nu_x Re_x^{-1/2})$ for the increase of Pr from 0.7 to 3.0 is approximately 250 % when $\lambda = 1$, $\lambda_1 = 0.1$, $A = 1$ and $\xi = 0.5$.

Fig. 7 displays the effect of rotational parameter (λ_1) on the velocity and temperature profiles (f_η, g). The velocity overshoot observed near the wall within the boundary layer as the slender cylinder rotates faster because the rotating slender cylinder cause rotation in the fluid near the wall within the boundary layer and rotating fluid with the buoyancy force moves faster near the wall within the boundary layer compared to the fluid away from the wall. In contrast, the velocity overshoot is not much significant when slender cylinder remains stationary ($\lambda_1 = 0$). The effect of rotational parameter (λ_1) on temperature profile is not much significant as shown in Fig. 7 because the rotational parameter (λ_1) is not present explicitly in the energy equation. The effects of buoyancy parameter (λ) and Prandtl number (Pr) on the velocity component in θ direction are not much because both of these parameters are not present explicitly in θ-momentum equation. The effects of injection ($A < 0$) and suction ($A > 0$) parameters on the velocity and temperature profiles are shown in Fig. 8. In case of injection, the fluid is carried away from the surface causing

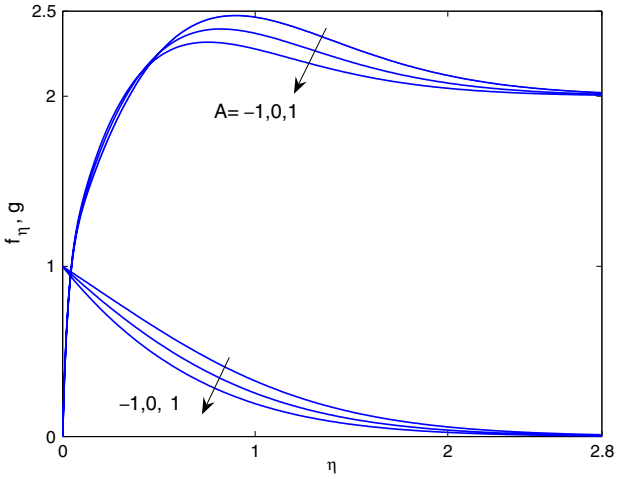

Fig. 8. Effect of A on the velocity and temperature profiles (f_η, g) when $\lambda = 1$, $\lambda_1 = 1$, $Pr = 0.7$ and $Re = 10^4$.

reduction in the velocity gradient as it tries to maintain the same velocity over a very small region near the surface, and this effect is reversed in the case of suction. The higher velocity overshoot is observed near the wall within the boundary layer for injection ($A < 0$) and overshoot is decreased for suction ($A > 0$). Injection ($A < 0$) causes a decrease in the steepness of the velocity profile (f_η) at the wall but the steepness of the velocity profile (f_η) increases with suction. The effects of injection ($A < 0$) and suction ($A > 0$) on the skin friction and heat transfer coefficients $(C_{fx} Re_x^{1/2}, C_{f\theta} Re_x^{1/2}, Nu_x Re_x^{-1/2})$ are shown in Fig. 9. As expected, results indicate that skin friction and heat transfer coefficients $(C_{fx} Re_x^{1/2}, C_{f\theta} Re_x^{1/2}, Nu_x Re_x^{-1/2})$ increase with the increase of suction ($A > 0$) but decrease as the magnitude of injection ($A < 0$) increase. Suction/injection parameters (A) have no effect on the skin friction coefficients and Nusselt number $(C_{fx} Re_x^{1/2}, C_{f\theta} Re_x^{1/2}, Nu_x Re_x^{-1/2})$ at $\xi = 0$ because the value of the non-dimensional stream functions

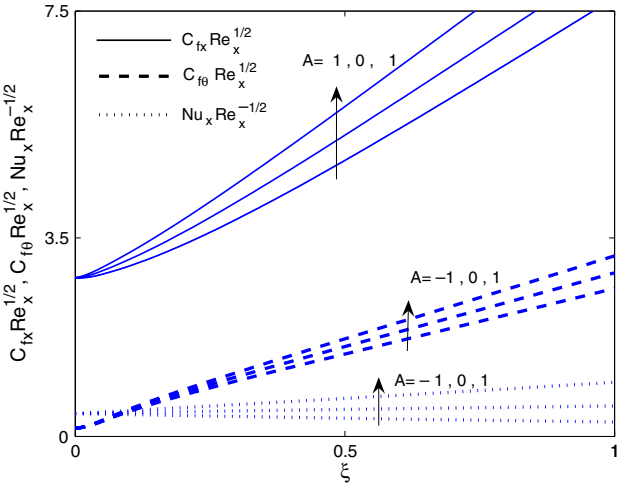

Fig. 9. Effect of A on the skin frictions and Nusselt number $(C_{fx}Re_x^{1/2}, C_{f\theta}Re_x^{1/2}, Nu_xRe_x^{-1/2})$ when $\lambda = 1$, $\lambda_1 = 0.1$, $Re = 10^4$ and $Pr = 0.7$.

at the wall is equal to A multiplied by ξ i.e., $f_w = A\xi$. For example, for $\lambda = 1$, $Pr = 0.7$, $\lambda_1 = 0.1$ and $\xi = 0.5$, Fig. 9 shows that the skin friction coefficients and Nusselt number $(C_{fx}Re_x^{1/2}, C_{f\theta}Re_x^{1/2}, Nu_xRe_x^{-1/2})$ increase approximately by the 19%, 16% and 100%, respectively, as the value of A changes from -1 to 1.

5. Conclusions

Non-similar solutions of a mixed convection flow along a vertical rotating slender cylinder with injection/suction have been obtained . The buoyancy force causes significant overshoot in the velocity profile for low Prandtl number fluid. The rotational parameter (λ_1) decreases the boundary layer thickness. The surface skin friction is strongly depend on the buoyancy force due to the thermal diffusion, and on the relative velocity between the wall and the free stream. The surface skin friction coefficients in x- and θ-directions increase with the buoyancy parameter and decrease with the increase of Prandtl number Pr. Skin friction coefficients in the x- and θ-direction and heat transfer rate are found to alter significantly due to injection/suction and buoyancy parameter λ.

References

[1] T.S. Chen, A. Mucoglu, Buoyancy effects on forced convection along a vertical cylinder, ASME J. Heat Transfer 97 (1975) 198–203.
[2] J.P. Narain, Free and forced convective heat transfer from slender cylinder, Lett. Heat Mass Transfer 3 (1976) 21–30.
[3] M.N. Bui, T. Cebeci, Combined free and forced convection on vertical slender cylinders, ASME J. Heat Transfer 107 (1985) 476–478.
[4] T.Y. Wang, C. Kleinstrever, General analysis of steady mixed convection heat transfer on vertical slender cylinders, ASME J. Heat Transfer 111 (1989) 393–398.
[5] J.J. Heckel, T.S. Chen, B.F. Armaly, Mixed convection along slender vertical cylinders with variable surface temperature, Int. J. Heat Mass Transfer 32 (1989) 1431–1442.
[6] H.S. Takhar, A.J. Chamkha, G. Nath, Combined heat and mass transfer along a vertical moving cylinder with a free stream, Heat Mass Transfer 36 (2000) 237–246.
[7] M. Kumari, G. Nath, Mixed convection boundary layer flow over a thin vertical cylinder with localised injection/suction and cooling/heating, Int. J. Heat Mass Transfer 47 (2004) 969–976.
[8] A. Ziabicki, Fundamentals of Fibre formation, Wiley, New York, 1976.
[9] H. Schlichting, Boundary Layer Theory, Springer, New York, 2000.
[10] R.E. Bellman, R.E. Kalaba, Quasilinearization and Non-linear Boundary value problem, Elsevier, USA, 1965.
[11] K. Inouye, A. Tate, Finite difference version quasilinearization applied to boundary layer equations, AIAAJ 12 (1974) 558–560.
[12] S. Roy, P. Saikrishnan, Non-uniform slot injection (suction) into steady laminar boundary layer flow over a rotating sphere, Int. J. Heat Mass Transfer 46 (2003) 3389–3396.
[13] R.S. Varga, Matrix Iterative Analysis, Printice Hall, 2000.